Population dynamics and phase effects in periodic level crossings

B. M. Garraway[1] and N. V. Vitanov[1,2]
[1]*Optics Section, Blackett Laboratory, Imperial College, Prince Consort Road, London SW7 2BZ, United Kingdom*
[2]*Research Institute for Theoretical Physics, P.O. Box 9, Siltavuorenpenger 20 C, University of Helsinki, 00014 Helsinki, Finland*
(Received 16 October 1996)

We present an analytic study of the population dynamics of a two-state system interacting with an external field and subjected to periodic level crossings. We apply an evolution matrix approach to calculate the excited-state population at the crossings (the nodes) and at the antinodes. The results are expressed in terms of only two parameters: the transition probability p for a quarter period from a crossing to an antinode, and the transition probability P for a half period between two successive crossings. We find that the values of the excited-state population at the antinodes can form global (gross) structures. We show that these structures and the population dynamics as a whole are very sensitive to the initial phase φ of the frequency-modulated field, particularly in the limits $\varphi=0$ (cosine modulation) and $\varphi=\pi/2$ (sine modulation). We calculate the parameters p and P by using two analytic approaches: one based on the original Landau-Zener model, and the other based on the finite Landau-Zener model. Both approaches unexpectedly lead to the same results. The notion of the global structures and the relevant parametrization in terms of p and P allow us to find various distinctive cases of population dynamics, such as population swapping, completely periodic evolution, superpositional trapping, and stepwise evolution. [S1050-2947(97)06806-6]

PACS number(s): 32.80.Bx, 33.80.Be, 42.50.−p

I. INTRODUCTION

The problem of a two-state system coupled to an external time-dependent field can be met in many areas in physics, such as magnetic resonance [1–3], laser-atom interactions [4], atomic collisions [5], solid-state physics [6], in chemistry [7] and even in biology [8]. Particular attention in the literature has been paid to the problems of a level crossing [1], noncrossing [2], adiabatic evolution and nonadiabatic transitions. It is, for instance, well known that in the adiabatic regime, a level crossing leads to a large transition probability while the absence of a crossing leads to no transitions. Less obvious is the population dynamics of a two-state system whose interaction with an external time-dependent field leads to repeated and periodic level crossings that produce multiple interference effects.

Periodic level crossings may arise in a number of problems, e.g., two-level atoms interacting with frequency-modulated laser light, transitions in a double-well potential due to an external harmonic field, atoms traveling in periodic structures, ions in traps, and mode dynamics in optical cavities. The problem has been a subject of considerable interest in recent years, particularly in studies on transitions in a double-well potential in solid-state physics [9–11], in quantum transport analysis [12] and in optical physics [13,14]. Among the results, we will mention an interesting effect called *coherent destruction of tunneling* in double-well potential studies [9,10], *dynamic localization* in transport analysis [12], and *population trapping* in laser-atom physics [14]. It consists of the suppression of transitions and takes place when the ratio between the modulation amplitude A and the modulation frequency ω is equal to a zero of the Bessel function $J_0(z)$ with the proviso that the modulation frequency ω is much larger than the coupling Ω. Attention has also been paid to the effect of dissipation on the population dynamics by using numerical methods [11,13,14] and simple approximate analytic models in the limit of strong dissipation [11,13]. In this latter case, a simplification arises from the loss of coherence between the crossings.

In this paper, we study analytically the population dynamics of a two-state system subjected to periodic level crossings by an external field in the absence of dissipation, that is, in the fully coherent limit. To be specific we will use the quantum optical terminology appropriate for a two-state atom coupled to frequency-modulated light. We develop an *evolution matrix approach* to periodic two-state systems that is a useful alternative to the standard Floquet theory. The evolution matrix approach enables us to identify *gross* (or *global*) *structures* in the time evolution of the system. These structures are formed from the values of the excited-state population at the antinodes, and result in features of the evolution on a short time scale (substructures) being repeated at regular intervals on a long time scale. Our results generalize and contain as particular cases some known results, such as the perturbative limit, and the adiabatic solution. We derive the conditions for new, exotic, types of time evolution and clarify the conditions for some cases discussed earlier. Furthermore, we establish the relationship between the periodic problem and the Landau-Zener model. We also demonstrate that the global structures and the population dynamics as a whole are very sensitive to the *initial phase* φ of the frequency-modulated field, particularly in the cases $\varphi=0$ and $\varphi=\pi/2$.

This paper is organized as follows. In Sec. II, we introduce the model and give the approximate solutions in two limiting cases: that of small coupling and in the adiabatic limit. In Sec. III, we present the evolution matrix approach, which provides the values of the excited-state population at the crossings (the nodes) and at the antinodes in terms of only two parameters: the transition probability p for a quarter period from a crossing to an antinode, and the transition probability P for a half period between two successive cross-

ings. This leads to a description of the global structures mentioned above. In Sec. IV, we calculate the parameters p and P by using two approaches based on the original Landau-Zener (LZ) model [1] and the finite Landau-Zener model [15]. In Sec. V, we apply the results to find various types of population dynamics, including population swapping, completely periodic evolution, superpositional trapping, stepwise evolution, and others. Finally, in Sec. VI, we present the conclusions.

II. DEFINITION OF THE PROBLEM AND LIMITING CASES

A. Definition of the problem

The time evolution of the probability amplitudes $\mathbf{c}(t)=(c_1(t),c_2(t))^T$ of a coherently driven nondissipative two-level system is governed by the Schrödinger equation, which in the interaction representation has the form

$$i\frac{d}{dt}\mathbf{c}(t)=\begin{bmatrix} 0 & \frac{1}{2}\Omega(t)e^{-iD(t)} \\ \frac{1}{2}\Omega(t)e^{iD(t)} & 0 \end{bmatrix}\mathbf{c}(t), \quad (1)$$

where the rotating-wave approximation (RWA) has been made and $D(t)=\int_0^t\Delta(t')dt'$. We assume that the (on-resonance) Rabi frequency $\Omega(t)$ and the detuning $\Delta(t)$ are given by

$$\Omega(t)=\begin{cases} 0, & \omega t<-\varphi \\ \Omega, & \omega t\geqslant-\varphi, \end{cases} \quad (2)$$

$$\Delta(t)=A\cos(\omega t),$$

that is, the laser field is turned on at time $t_0=-\varphi/\omega$ and kept constant while the detuning has a sinusoidal behavior, thus leading to repeated and periodic crossings of the resonance, as shown in Fig. 1. The problem is equivalent to and leads to the same results as the model with a coupling turned on at $t_0=0$ and detuning $\Delta(t)=A\cos(\omega t-\varphi)$, which is also shown in Fig. 1, but the definition (2) leads to simpler derivations. We suppose that the system is initially in its ground state,

$$c_1(-\varphi/\omega)=1, \quad c_2(-\varphi/\omega)=0, \quad (3)$$

and we are interested in the excited-state population at time t, $P_\varphi(\omega t)=|c_2(t)|^2$. The problem is characterized by three parameters with the dimension of frequency Ω, A, and ω. Insofar as the populations are dimensionless, they must depend on the ratios of these frequencies. Among the three possible ratios only two are independent and we choose these to be A/ω and Ω/ω. Furthermore, we will use the dimensionless time ωt in the evolution matrices and the populations throughout the paper. In other words, we choose the modulation frequency ω to determine the frequency and time scales of our problem. Simple solutions exist in two particular extreme cases: that of *small coupling* ($\Omega/\omega\ll1$) and in the *adiabatic limit* ($\Omega^2\gg A\omega$). These cases are schematically shown in Fig. 2 and we will consider them below.

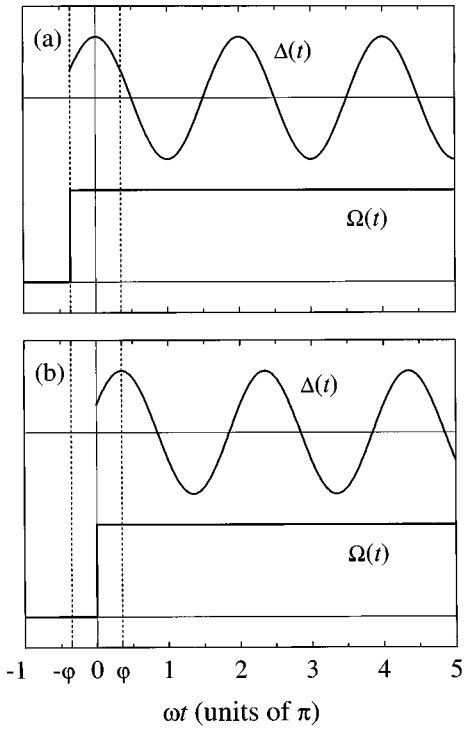

FIG. 1. (a) The model (2) studied in this paper. The laser field is turned on at time $t_0=-\varphi/\omega$ and kept constant while the detuning has a sinusoidal behavior, leading to repeated and periodic crossings of the resonance. (b) The equivalent problem of a coupling turned on at $t_0=0$ and detuning $\Delta(t)=A\cos(\omega t-\varphi)$.

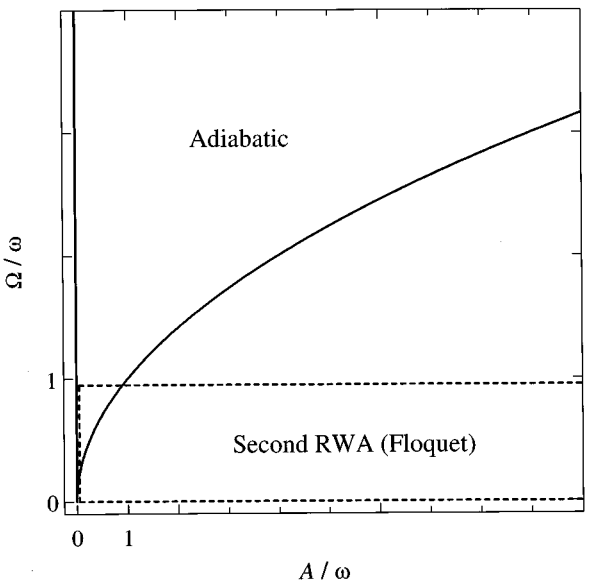

FIG. 2. Schematic representation of the region of validity of the *second rotating-wave approximation* (small coupling, $\Omega/\omega\ll1$) whose boundaries are shown by the dashed line and which is discussed in Sec. II B, and the region of validity of the *adiabatic solution* [$(\Omega/\omega)^2\gg A/\omega$] presented in Sec. II C, whose boundaries are depicted by the solid curve. Note that the regions shown [$\Omega/\omega<1$ and $(\Omega/\omega)^2>A/\omega$] are larger than the actual regions [$\Omega/\omega\ll1$ and $(\Omega/\omega)^2\gg A/\omega$].

B. Small coupling ($\Omega/\omega \ll 1$)

This case has been well studied and understood in the last few years by means of the Floquet formalism [9,11,12,14]. We summarize it here for the sake of completeness and in order to emphasize later the differences between its features and those in the other regimes. Since $D(t) = \int_0^t \Delta(t')dt' = (A/\omega)\sin(\omega t)$, we can expand the exponents in Eq. (1) in terms of Bessel functions by using the relation [16]

$$e^{iz\sin\gamma} = \sum_{n=-\infty}^{\infty} e^{in\gamma} J_n(z).$$

Thus we obtain

$$\frac{1}{2}\Omega e^{iD(t)} = \frac{1}{2}\Omega \sum_{n=-\infty}^{\infty} e^{in\omega t} J_n(A/\omega). \tag{4}$$

When $\omega \gg \Omega$, only the nonoscillating term with $n=0$ in the sum contributes significantly to the population evolution. By neglecting all other terms (which is equivalent to a *second rotating-wave approximation*), one finds that the excited-state population is given by

$$P_\varphi(\omega t) \approx \sin^2\left[\frac{\Omega}{2\omega} J_0(A/\omega)(\omega t + \varphi)\right] + O(\Omega/\omega) \quad (\Omega \ll \omega). \tag{5}$$

This result is valid for any modulation amplitude A. Equation (5) suggests that if A/ω is equal to one of the zeroes of $J_0(A/\omega)$ [denoted usually by $j_{0,k}$ $(k=1,2,3,\ldots)$], then the excited-state population is approximately zero. This effect has been called *coherent destruction of tunneling* in studies on tunneling in a double-well potential [9], *dynamic localization* in quantum transport theory [12], and *population trapping* in optical physics [14]. Moreover, we have to stress that the phase φ does *not* affect substantially the population evolution and, as Eq. (5) shows, it only shifts the time scale.

Evidently, this effect is strictly valid in the second RWA only. For $A/\omega = j_{0,k}$, we can estimate the excited-state population by keeping the terms with odd $n = \pm 1, \pm 3, \ldots$ in Eq. (4) and neglecting those with even n. Then, since $J_{-n}(z) = (-1)^n J_n(z)$, the sum in Eq. (4) is purely imaginary. Equations (1) are easily solved and we find

$$P_\varphi(\omega t) \approx \sin^2\left\{\frac{\Omega}{\omega}\sum_{m=0}^{\infty} \frac{J_{2m+1}(j_{0,k})}{2m+1}[\cos(2m+1)\omega t - \cos(2m+1)\varphi]\right\} \quad (\Omega \ll \omega \text{ and } A/\omega = j_{0,k}). \tag{6}$$

Obviously, $P_\varphi(\omega t)$ is small due to $\Omega \ll \omega$ and it oscillates between 0 and its maximum value, which is of order $O(\Omega^2/\omega^2)$. Note that for $A/\omega \neq j_{0,k}$, the solution (5) oscillates between 0 and 1. When $A/\omega = j_{0,k}$ is large, Eq. (6) should be a good approximation because, as the asymptotics [16]

$$J_\nu(z) \sim \sqrt{2/(\pi z)}\cos\left(z - \frac{1}{2}\pi\nu - \frac{1}{4}\pi\right) \quad (\nu \text{ fixed}, |z| \to \infty) \tag{7}$$

shows, the zeros of $J_{2m}(z)$ are close to the zeros of $J_0(z)$ and hence, $J_{2m}(j_{0,k}) \approx 0$. Although rather simple, formula (6) has not, apparently, appeared in the literature so far.

C. Adiabatic limit ($\Omega^2 \gg A\omega$)

The adiabatic evolution is realized when the system follows one of the eigenstates (adiabatic states) of the Hamiltonian. This takes place when the nonadiabatic coupling $\frac{1}{2}\dot{\vartheta}$ is much smaller than the eigenvalue splitting $\frac{1}{2}\Omega_0$ (Appendix A), i.e., $|\dot{\vartheta}| \ll \Omega_0$, where

$$\tan\vartheta = \frac{\Omega}{\Delta} \quad (0 \leq \vartheta \leq \pi), \tag{8}$$

$$\Omega_0 = \sqrt{\Omega^2 + \Delta^2}. \tag{9}$$

The adiabatic condition in our problem is least well satisfied at the crossings ($\Delta = 0$), where it requires

$$\Omega^2 \gg A\omega. \tag{10}$$

The adiabatic solution is, of course, well known. For the reader's convenience, it is given in Appendix A. Provided the population is in the ground state at time t_0, the excited-state population at time t in the adiabatic limit is

$$P_\varphi^{\mathrm{ad}}(\omega t) \approx \frac{1}{2} - \frac{\Delta(t)\Delta(t_0)}{2\Omega_0(t)\Omega_0(t_0)} - \frac{\Omega(t)\Omega(t_0)}{2\Omega_0(t)\Omega_0(t_0)}\cos 2\phi_{\mathrm{ad}}(\omega t, \omega t_0), \tag{11}$$

where

$$\phi_{\mathrm{ad}}(\omega t_0, \omega t) = \frac{1}{2}\int_{t_0}^{t} \Omega_0(t')dt' \tag{12}$$

is the adiabatic phase acquired between times t_0 and t. It is clear from Eq. (11) that the population evolution is characterized by two time scales. There is a fast time scale determined by the last term that generates rapid oscillations. In the Bloch vector representation of a two-state state system this is caused by the rapid precession of the Bloch vector about a pseudomagnetic field vector. The slow time scale is determined by the second term, which causes slow precession. In the Bloch vector picture, the pseudomagnetic field vector slowly moves about, carrying the precessing Bloch vector with it. The ensuing modulation of any projection of

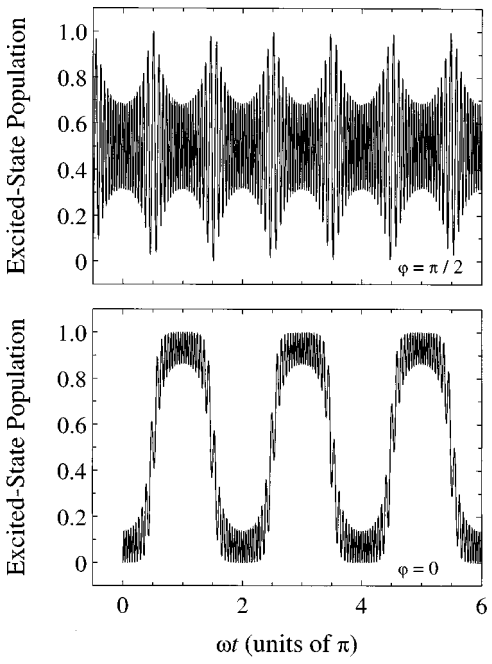

FIG. 3. A case of almost perfect adiabatic evolution ($\Omega/\omega=20, A/\omega=50$). Upper figure, $\varphi=\pi/2$; lower figure, $\varphi=0$. The adiabatic solution (11) (not shown) coincides almost completely with the exact numerical results.

the Bloch vector (such as populations) corresponds to elements of the *global structures* introduced in the next section.

It is worthwhile pointing out that in contrast to the case of small coupling, considered in Sec. II B, in the adiabatic regime the initial phase φ *can* alter the population dynamics significantly because $\Delta(t_0)$ is different. For example, if $\varphi=0$, the initial value of the detuning $\Delta(t_0=0)=A$ is maximal and the precession amplitude is maximal too, but if $\varphi=\pi/2$, we have $\Delta(t_0=-\varphi/\omega)=0$ and there is no slow precession [from the second term in Eq. (11)]. On the other hand, for cosine modulation ($\varphi=0$) and $A\gg\Omega$ [the condition (10) can still be satisfied if both A/ω and Ω/ω are large], then near the antinodes ($\Delta\approx A$) the third term in (11) is much smaller than the second one, which approaches $\frac{1}{2}$. Hence, depending on the sign of $\Delta(t)$, the population around the antinodes resides either in the ground or in the excited state almost completely. This is the regime of *population swapping*, which will be discussed later on. Such a case is shown in Fig. 3. Note that this effect cannot take place for sine modulation ($\varphi=\pi/2$). Finally, we should point out that as Eq. (11) shows, and in agreement with earlier conclusions [17], adiabatic evolution and a level crossing do not necessarily lead to a diabatic transition probability of unity, unless the ratio Δ/Ω diverges at the initial and the final times.

For $1<\Omega^2/\omega^2<A/\omega$, neither the Floquet analysis from Sec. II B nor the adiabatic solution apply. In the next section we develop a completely different approach to treat the general case. Following the discussion of the adiabatic regime, we will separate the population evolution into two parts, or in other words, we will distinguish two time scales. The *local* behavior (the short time scale) can be deduced from the knowledge compiled on two-level systems, which suggests that the biggest changes in the populations (''jumps'') must occur around the crossings (the nodes) while between them (around the antinodes) one is to expect Rabi-like oscillations. The *global structure* (exhibited on a longer time scale) is a feature that will be discussed in more detail below. It emerges when we consider the curves on which the values of the populations at the antinodes lie. We will be mainly concerned with the two limiting cases, $\varphi=0$ and $\varphi=\pi/2$, as they lead to the most extreme differences in the population evolution.

III. EVOLUTION MATRIX APPROACH AND GLOBAL STRUCTURES

A. Evolution matrix approach

The approach we choose to treat the global structures for $\varphi=0$ (cosine modulation) and $\varphi=\pi/2$ (sine modulation) consists of several steps: (i) we separate the entire evolution into intervals of length $\pi/2$ (quarter periods); (ii) we express the evolution matrix for any quarter-period interval in terms of the evolution matrix $\mathbf{U}(\pi/2,0)$ for the interval $[0,\pi/2]$; (iii) we find the evolution matrix for the entire evolution from ωt_0 to the Nth node or antinode by matrix multiplication of the evolution matrices for the preceding intervals.

By definition, $\mathbf{c}(t)=\mathbf{U}(\omega t,\omega t_0)\mathbf{c}(t_0)$. Let us denote the basic evolution matrix in the interval $[0,\pi/2]$ by $\mathbf{U}\equiv\mathbf{U}(\pi/2,0)$. Since it is a unitary matrix, it can be parametrized by

$$\mathbf{U}\equiv\mathbf{U}(\pi/2,0)=\begin{bmatrix}\sqrt{1-p}\,e^{i(\eta+\zeta)/2} & \sqrt{p}\,e^{-i(\eta-\zeta)/2}\\ -\sqrt{p}\,e^{i(\eta-\zeta)/2} & \sqrt{1-p}\,e^{-i(\eta+\zeta)/2}\end{bmatrix}, \tag{13}$$

where p is the transition probability in $[0,\pi/2]$ while η and ζ are dynamical phases. In order to find the evolution matrix for any interval in terms of $\mathbf{U}$ we need the following relations, which can readily be deduced from Eqs. (1):

$$\mathbf{U}(0,-\pi/2)=\mathbf{U}^T, \tag{14}$$

$$\mathbf{U}(\pi,\pi/2)=\sigma_3\mathbf{U}^\dagger\sigma_3, \tag{15}$$

$$\mathbf{U}(3\pi/2,\pi)=\sigma_3\mathbf{U}^*\sigma_3, \tag{16}$$

$$\mathbf{U}(\varphi_2+2\pi,\varphi_1+2\pi)=\mathbf{U}(\varphi_2,\varphi_1), \tag{17}$$

where σ_3 is the Pauli matrix

$$\sigma_3=\begin{bmatrix}1 & 0\\ 0 & -1\end{bmatrix}.$$

For example, we will need the transition probability in the interval $[-\pi/2,\pi/2]$, which is given by $P\equiv|U_{12}(\pi/2,-\pi/2)|^2$. Using relation (14) we find

$$\mathbf{U}(\pi/2,-\pi/2)=\mathbf{U}\mathbf{U}^T. \tag{18}$$

In terms of the parameters of $\mathbf{U}$ [see Eq. (13)], P is given by

$$P=4p(1-p)\,\sin^2\eta. \tag{19}$$

It is possible to express the values of the populations at the antinodes $\omega t=N\pi$ and at the crossings $\omega t=(N+\frac{1}{2})\pi$ in

terms of the transition probabilities p and P only. The evolution-matrix elements at these points are derived in Appendix B for cosine ($\varphi=0$) and sine ($\varphi=\pi/2$) modulation. Given the initial conditions (3), the excited-state population is equal to the squared modulus of the off-diagonal element of the corresponding evolution matrix. The values of the excited-state population at the antinodes form the global structures.

B. Excited-state population at the antinodes: global structures

For *cosine modulation* ($\varphi=0$), the excited-state population at the even (top) antinodes $\omega t=0,2\pi,4\pi,\ldots$ is [cf. Eq. (B5)]

$$P_{\varphi=0}(2N\pi)=\frac{(1-2p)^2}{1-P}\sin^2(N\beta)\quad(N=0,1,2,\ldots) \tag{20}$$

while at the odd (bottom) antinodes $\omega t=\pi,3\pi,5\pi,\ldots$ it is [cf. Eq. (B7)]

$$P_{\varphi=0}[(2N+1)\pi]=1-\frac{(1-2p)^2}{1-P}\cos^2\left[\left(N+\frac{1}{2}\right)\beta\right] \tag{21}$$

$$(N=0,1,2,\ldots),$$

where

$$\cos\beta=1-2P\quad(0\leqslant\beta\leqslant\pi). \tag{22}$$

The points $P_{\varphi=0}(2N\pi)$ $(N=0,1,2,\ldots)$ form an *''even'' global structure* $G^{e}_{\varphi=0}(\omega t)$ and the points $P_{\varphi=0}[(2N+1)\pi]$ $(N=0,1,2,\ldots)$ form another *''odd'' global structure* $G^{o}_{\varphi=0}(\omega t)$. By replacing $2N\pi$ by ωt in Eq. (20) and $(2N+1)\pi$ by ωt in Eq. (21) we obtain the equations for these global structures

$$G^{e}_{\varphi=0}(\omega t)=\frac{(1-2p)^2}{1-P}\sin^2\left(\frac{\beta}{2\pi}\omega t\right), \tag{23}$$

$$G^{o}_{\varphi=0}(\omega t)=1-\frac{(1-2p)^2}{1-P}\cos^2\left(\frac{\beta}{2\pi}\omega t\right). \tag{24}$$

Therefore, for cosine modulation, there are *two* global structures, which are two *in-phase* sinusoids with periods of $2\pi^2/\beta$ shifted with respect to each other by the (constant) splitting

$$G^{o}_{\varphi=0}(\omega t)-G^{e}_{\varphi=0}(\omega t)=1-\frac{(1-2p)^2}{1-P}\geqslant 0. \tag{25}$$

Note that the upper structure $G^{o}_{\varphi=0}(\omega t)$ comprises the bottom (odd) antinodes.

For *sine modulation* ($\varphi=\pi/2$), the excited-state population at the top antinodes $0,2\pi,4\pi,\ldots$ is [cf. Eq. (B9)]

$$P_{\varphi=\pi/2}(2N\pi)=\frac{1}{2}-\frac{1-2p}{2\sqrt{1-P}}\cos\left[\left(2N+\frac{1}{2}\right)\beta\right] \tag{26}$$

$$(N=0,1,2,\ldots),$$

while the excited-state population at the bottom antinodes $\pi,3\pi,5\pi,\ldots$ is [cf. Eq. (B11)]

$$P_{\varphi=\pi/2}[(2N+1)\pi]=\frac{1}{2}-\frac{1-2p}{2\sqrt{1-P}}\cos\left[\left(2N+\frac{3}{2}\right)\beta\right] \tag{27}$$

$$(N=0,1,2,\ldots).$$

By replacing $2N\pi$ by ωt in Eq. (26) and $(2N+1)\pi$ by ωt in Eq. (27) we conclude that for sine modulation, there is only *one* global structure comprising the values of the excited-state population at both the top and the bottom antinodes. This gross structure is defined by

$$G_{\varphi=\pi/2}(\omega t)=\frac{1}{2}-\frac{1-2p}{2\sqrt{1-P}}\cos\left[\left(\frac{\omega t}{\pi}+\frac{1}{2}\right)\beta\right] \tag{28}$$

and its period is $2\pi^2/\beta$, the same as the period of the global structures for cosine modulation. It can be shown that this is the period of the global structures for any φ.

The implication from the above results is that if the jumps at the crossings are small enough, the global excitation history for sine modulation is a *stepwise* trajectory. For cosine modulation, the global evolution is more complicated and, depending on the splitting (25), can either consist of alternative *upward and downward jumps* or be a stepwise trajectory as for sine modulation. More detailed discussion on the behavior of the global structures follows in Sec. V.

We should particularly emphasize that in contrast to the regime of small coupling (Sec. II B), in the general case the population dynamics is quite sensitive to the initial phase φ. In Fig. 4, we have shown the population evolution for several values of φ in the range $[0,\pi/2]$. The population evolution when φ is in the range $[\pi/2,\pi]$ looks similar, although it is not completely the same. Moreover, it is clear from Eqs. (2) that the population evolution for φ is the same (up to a shift in the time scale) as for $\varphi+k\pi$ $(k=0,\pm1,\pm2,\ldots)$. Figure 4 shows that the population history is nearly the same in the range $0\leqslant\varphi\leqslant 0.45\pi$ and then rapidly changes as φ approaches $\pi/2$. This is because the case of arbitrary φ can be viewed as cosine modulation ($\varphi=0$) but with some preexcitation in the interval $[-\varphi,0]$, i.e., as cosine modulation with the system being initially (at $t=0$) in a coherent superposition of states rather than in a single state. This ''preexcitation'' is strongest if the laser field is turned on near the crossing where the populations change most significantly, that is when $\varphi\approx\pi/2$. We should also emphasize that for any $\varphi\neq\pi/2$ there are two global structures that ultimately degenerate into one for $\varphi=\pi/2$. This can be easily seen from the expression

$$\frac{4p(1-p)(1-2p)}{1-P}\cos\eta\left[\frac{1-2p_\varphi}{1-2p}\cos\eta-\sqrt{\frac{p_\varphi(1-p_\varphi)}{p(1-p)}}\cos\eta_\varphi\right],$$

which gives the splitting between the two global structures for arbitrary φ. It can be found in a similar way to the derivations for $\varphi=0$ and $\varphi=\pi/2$ in Appendix B. The transition

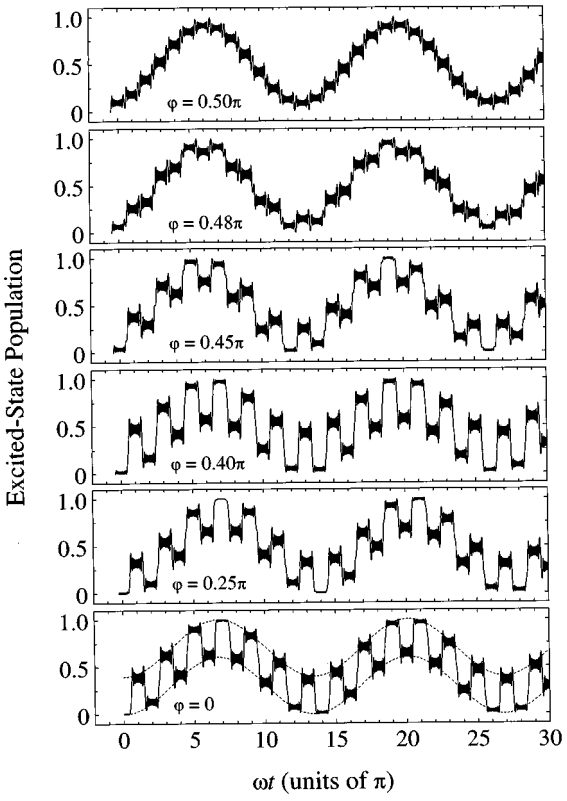

FIG. 4. The excited-state population evolution for $\Omega/\omega=3$ and $A/\omega=33$ and several values of φ (denoted on the figures). The dashed curves for $\varphi=0$ are the global structures (23) and (24).

probability p_φ and the dynamic phase η_φ are defined similarly to Eq. (13) but for the interval $[0,\varphi]$. Evidently, the splitting vanishes only for $p_\varphi=p$ and $\eta_\varphi=\eta$, i.e., for $\varphi=\pi/2$, except in some incidental cases.

It is readily seen that in the limit of small coupling ($\Omega\ll\omega$), and for the specific case of $\Delta(t)=A\cos\omega t$ [Eq. (2)], the global structures (23), (24), and (28) reduce to the weak coupling result (5). Consider, for example, the case of cosine modulation ($\varphi=0$). For weak excitation we have $p\ll1$, $P\ll1$, and the two global structures (23) and (24) coalesce into one, $G_{\varphi=0}(\omega t)\approx\sin^2(\beta\omega t/2\pi)$. To estimate $\beta=\arccos(1-2P)\approx2\sqrt{P}$, we use perturbation theory to find

$$P\approx\left|-\frac{i}{2}\Omega\int_{-\pi/2\omega}^{\pi/2\omega}e^{i(A/\omega)\,\sin\omega t}dt\right|^2=\left[\frac{\pi\Omega}{2\omega}J_0(A/\omega)\right]^2, \tag{29}$$

with the help of Eq. (9.1.18) of Ref. [16]. Hence, $\beta\approx(\pi\Omega/\omega)J_0(A/\omega)$, which leads to $G_{\varphi=0}(\omega t)\approx\sin^2[\frac{1}{2}J_0(A/\omega)\Omega t]$, which is exactly Eq. (5) for $\varphi=0$. Thus, the global structures, which in general comprise only the values of the excited-state population at the antinodes, give the correct excited-state population at any t in the limit of weak excitation, $\Omega\ll\omega$, irrespective of the value of A.

Finally, we should point out that Eqs. (20)–(28) are exact. Related approximate results have been reported in Ref. [11] for the specific case of cosine modulation, $\Delta(t)=A\cos\omega t$, in the limit $A\gg\Omega,\omega$.

C. Excited-state population at the nodes

For *cosine modulation* ($\varphi=0$) the excited-state population at the nodes $\omega t=\pi/2,3\pi/2,5\pi/2,\ldots$ is

$$P_{\varphi=0}\left[(2N+1)\frac{\pi}{2}\right]=\frac{1}{2}-\frac{1-2p}{2\sqrt{1-P}}\cos\left[(2N+1)\frac{\beta}{2}\right]$$

$$(N=0,1,2,\ldots) \tag{30}$$

while for *sine modulation* ($\varphi=\pi/2$) it is

$$P_{\varphi=\pi/2}\left[(2N+1)\frac{\pi}{2}\right]=\sin^2\left[(2N+1)\frac{\beta}{4}\right]\quad(N=0,1,2,\ldots). \tag{31}$$

These results can be derived in a similar manner as Eqs. (20), (21), (26), and (27). Thus, the excited-state populations at the crossings lie on just *one* sinusoid for cosine modulation and on another sinusoid for sine modulation. These sinusoids are less noticeable compared to the global structures that comprise the antinodes because at the crossings the excited-state population ''jumps'' up or down and the crossing points lie nearly in the middle of these jumps.

Finally, we should stress that all results derived in this section apply not only for the sinusoidal modulation (2) but for *any kind of periodic detuning modulation* with a period of 2π, provided the detuning is symmetric in $[0,\pi]$ and antisymmetric in $[0,2\pi]$. Of course, the particular values of p and P depend on the specific shape of the modulation. In the next section, we derive analytic approximations for p and P for the sinusoidal modulation (2), which is the most natural one. Nonetheless, the methods used by us can easily be applied to other modulations too.

IV. ANALYTIC DETERMINATION OF p AND P

We have developed two analytic approaches for the determination of the parameters p and P. The first is based on the finite Landau-Zener model [15] and the second is based on the original LZ model [1].

A. Approach based on the *finite* Landau-Zener model

We begin with the approach based on the *finite LZ model* and the calculation of p. We separate the time evolution within a quarter-period from the crossing to the adjacent antinode into two parts: from the crossing to a certain time T, and from T to the antinode, with T being a free matching parameter. In the interval from the crossing to T, the detuning $\Delta(t)$ is almost linear; thus, we calculate the evolution matrix by using the half-crossing finite LZ model [15] in order to account for nonadiabatic transitions. In the interval from T to the antinode we assume that the evolution is adiabatic and we use the adiabatic-following solution (Appendix A). The details of the derivation are given in Appendix C. The total evolution matrix for the quarter period [which in our approach is not $\mathbf{U}$ but rather $\mathbf{U}^T\mathbf{M}$; see Appendix C and Eq. (C1)] is a product of the adiabatic and the finite-LZ matrices and p is given by the squared modulus of the off-

diagonal element. The evolution matrix that gives the other probability P is $\mathbf{M}^*\mathbf{U}\mathbf{U}^T\mathbf{M}$. The approximate expressions obtained for p and P are

$$p \approx \tfrac{1}{2}[1-\cos\chi\,\cos\Theta-\sin\chi\sin\Theta\,\cos(\phi+2\phi_{\rm ad})], \quad (32)$$

$$P \approx \sin^2\chi\,\sin^2(\phi+2\phi_{\rm ad}) \quad (33)$$

with

$$\cos\chi = e^{-\pi\alpha^2/2} \quad (0\leqslant\chi\leqslant\pi/2), \quad (34)$$

$$\Theta \equiv \vartheta(\pi/2) = \arctan\frac{\Omega}{A} \quad (0\leqslant\Theta\leqslant\pi/2), \quad (35)$$

$$\phi(\alpha) = \arg\Gamma(1-i\alpha^2/2) + \frac{\pi}{4} + \frac{\alpha^2}{2}\left(\ln\frac{\alpha^2}{2}-1\right), \quad (36)$$

$$\phi_{\rm ad} \equiv \phi_{\rm ad}(0,\pi/2) = \frac{1}{2}\int_0^{\pi/2\omega}\sqrt{\Omega^2+A^2\,\cos^2\omega t}\,dt$$

$$= \frac{\sqrt{\Omega^2+A^2}}{2\omega}E(\cos\Theta), \quad (37)$$

where $E(k)$ is the complete elliptic integral of the second kind [16] and $\alpha=\Omega/\sqrt{2A\omega}$. The Landau-Zener phase $\phi(\alpha)$ is equal to $\pi/4$ at $\alpha=0$ and monotonically decreases to zero as $\alpha\to\infty$. In the derivation we have made two further approximations. We have replaced the Landau-Zener adiabatic phase $\phi_{\rm LZ}$ (C6) (i.e., for a linear detuning) accumulated from the crossing to T with the actual adiabatic phase $\phi_{\rm ad}$ accumulated in the same interval. Moreover, we have replaced the angle $\vartheta_{\rm LZ}(\omega T)$ of the rotation, which connects the diabatic and the adiabatic representations for the finite LZ model at the matching time T, by the angle $\vartheta(\omega T)$ (8) having the same role in the actual model (2). These changes, which actually correspond to matching in the adiabatic basis (A2) rather than in the diabatic one (A1), simplify the results and also eliminate the dependence on the matching time T.

It is readily seen by setting $\cos\chi=0$, $\sin\chi=1$, and $\phi=0$ that Eqs. (32) and (33) have the correct adiabatic limits ($\Omega^2\gg A\omega$) derived when Eq. (11) is applied in the corresponding intervals $[0,\pi/2]$ and $[-\pi/2,\pi/2]$, namely,

$$p_{\rm ad} \approx \frac{1}{2} - \frac{\Omega}{2\sqrt{\Omega^2+A^2}}\cos 2\phi_{\rm ad}, \quad (38)$$

$$P_{\rm ad} \approx \sin^2 2\phi_{\rm ad}. \quad (39)$$

Another useful check of the validity of our results can be carried out in the limit of weak excitation, $\Omega\ll\omega$, where we have already calculated the value of P perturbatively, Eq. (29). In this limit, the condition of validity of Eqs. (32) and (33) require $A\gg\omega$ [cf. condition (40) below]. For $\Omega\ll\omega\ll A$, we have $\sin^2\chi\approx\pi\Omega^2/(2A\omega)$, $\phi\approx\pi/4$, $\phi_{\rm ad}\approx A/2\omega$, and thus, our equation (33) gives $P\approx[\pi\Omega^2/(2A\omega)]\sin^2(A/\omega+\pi/4)$. This is indeed the correct limit obtained from Eq. (29) for $A\gg\omega$ by using the Bessel function asymptotics (7).

In Fig. 5, we compare formula (32) for p with the exact values derived numerically. In Fig. 6, we do the same with formula (33) for P . The purely adiabatic solutions (38) and (39) are also given. Formulas (32) and (33) are very accurate almost everywhere except when Ω/ω and A/ω are both small.

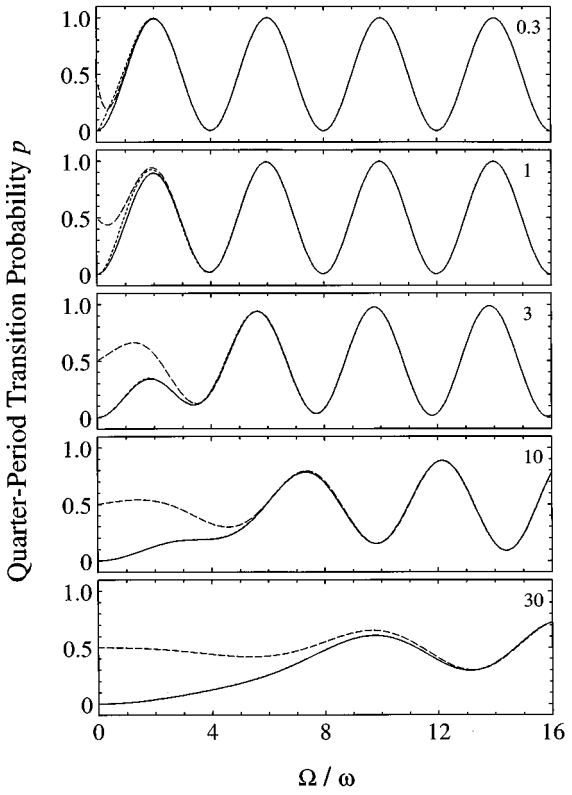

FIG. 5. The parameter p, representing the quarter-period transition probability from an antinode to a crossing, plotted as a function of the dimensionless ratio Ω/ω for several values of the ratio A/ω (denoted on the figures). The solid curves show the exact numerical results, the short-dashed curves show the analytic approximation (32) (which coincide with the solid curves almost everywhere except in the top two figures) and the long-dashed curves show the adiabatic solution (38).

B. Approach based on the *original* Landau-Zener model

We have also determined p and P by using the *original LZ model* instead of the finite LZ model. This cannot be done directly for a quarter period (for p) and a half period (for P) because there is no complete level crossing but only half crossings in these time intervals. Instead, we have determined p and P indirectly by considering the evolution between two successive antinodes as described in Appendix D. We have assumed that the evolution is purely adiabatic throughout except at the crossing where instantaneous nonadiabatic LZ transitions take place. Quite unexpectedly, the results are given again by Eqs. (32) and (33).

C. Discussion

The fact that both approaches lead to the same results is a little surprising given that their conditions of validity are supposed to be different. In the *finite LZ* approach (with the assumption for the moment that the matching point is in the middle of the quarter-period interval, $\omega T=\pi/4$), the validity conditions are

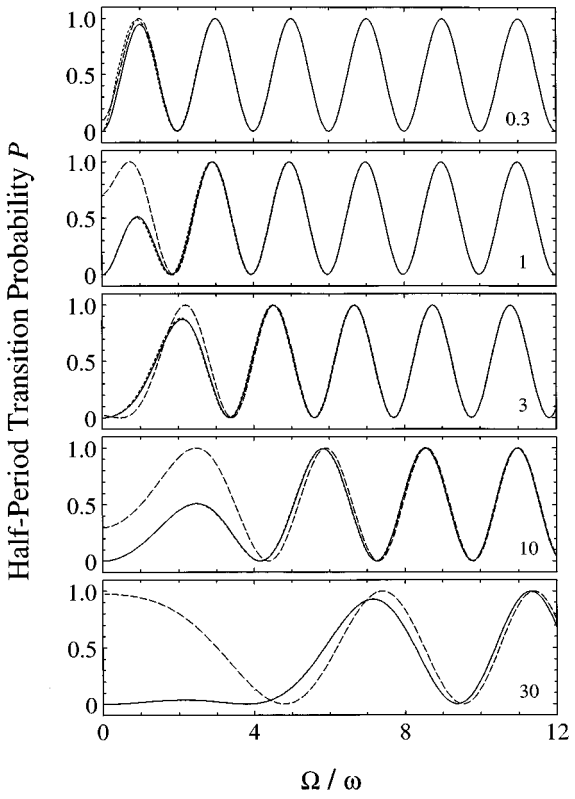

FIG. 6. The parameter P, representing the half-period transition probability between two successive crossings, plotted as a function of the dimensionless ratio Ω/ω for several values of the ratio A/ω (denoted on the figures). The solid curves show the exact numerical results, the short-dashed curves show the analytic approximation (33) (which almost coincide with the solid curves) and the long-dashed curves show the adiabatic solution (39).

$$\Omega^2+(\pi A/4)^2\gg 2A\omega,$$

$$(2\Omega^2+A^2)^{3/2}\gg 2\Omega A\omega.$$

The former ensures the validity of the asymptotic expansions used in the finite LZ model while the latter ensures the adiabatic evolution. These conditions generally require that Ω/ω and/or A/ω should be large, which can conveniently be written as

$$\Omega^2+A^2\gg\omega^2. \tag{40}$$

As Figs. 5 and 6 suggest, the condition (40) should be both necessary and sufficient for the validity of (32) and (33). Obviously, the finite LZ approach can only fail when Ω/ω and A/ω are both small, as is also confirmed by Figs. 5 and 6.

In the *original LZ* approach we have assumed that the evolution is purely adiabatic between the crossings while at each crossing instantaneous nonadiabatic LZ transitions take place. The restrictions on A/ω and Ω/ω that follow from these assumptions are much more stringent compared to condition (40). For instance, the adiabaticity between the crossings requires that $\Omega^2\gg A\omega$ while the instantaneous transitions impose a very small LZ transition time t_c, well within a half period: i.e., $t_c\ll\pi/\omega$. For nearly adiabatic excitation, the transition time in the diabatic basis (1) is $t_c\approx\Omega/(A\omega)$ [18], and this leads to the condition $\Omega/A\ll 1$. Thus, the conditions of validity of the original LZ approach seem to be

$$(\Omega/\omega)^2\gg A/\omega\gg\Omega/\omega\gg 1, \tag{41}$$

which are obviously much more restrictive than (40). For instance, the original LZ method is not expected to be valid for $\Omega/\omega>A/\omega\gg 1$ and for $A/\omega>(\Omega/\omega)^2\gg 1$, while it actually is. The fact that the original LZ method produces the correct result even where it is not supposed to work, i.e., that the actual conditions of validity are much more relaxed than the ''apparent'' conditions (41), is related to the nature of the Landau-Zener model. One of the reasons is that the transition time in the adiabatic basis (where the matching of the LZ solution to the adiabatic solution is actually made) may be shorter than t_c; in fact the value $\Omega/(A\omega)$, which is the width of the nonadiabatic coupling $\dot{\vartheta}$ (see Appendix A), gives only an *upper* limit for the transition time; i.e., the condition $\Omega/A\ll 1$ is too strong. This time is really shorter, which is related to the fact that the original LZ model produces the correct leading term of the finite LZ asymptotics in the adiabatic basis (A2). On the other hand, the requirement for adiabatic evolution throughout the interval between the crossings is also too strong because the condition for small transition time implies to a great extent that the nonadiabatic transitions are localized around the crossings anyway. The full discussion of this interesting issue, however, lies outside the scope of the present paper.

V. TYPES OF POPULATION DYNAMICS

The notion of the global structures developed in Sec. III and the relevant parametrization in terms of p and P allow us to find various distinctive cases of population dynamics, which are discussed below.

A. Population swapping ($p=\frac{1}{2}$)

When $p=\frac{1}{2}$, the global structures (23), (24), and (28) degenerate into horizontal straight lines. For cosine modulation ($\varphi=0$) we have $P_{\varphi=0}(2N\pi)=0$ and $P_{\varphi=0}[(2N+1)\pi]=1$, while for sine modulation ($\varphi=\pi/2$) we obtain $P_{\varphi=\pi/2}(N\pi)=\frac{1}{2}$. Hence, for $\varphi=0$ we expect the appearance of a regime of *complete population swapping*, the population being entirely either in the ground state (for $\omega t=2N\pi$) or in the excited state [for $\omega t=(2N+1)\pi$]. The curves in the parameter plane $(\Omega/\omega,A/\omega)$ on which $p=\frac{1}{2}$, can be found from our analytic approximation (32), which leads to the nonlinear equation

$$\cos(\phi+2\phi_{\rm ad})\approx-\frac{A}{\Omega\sqrt{e^{\pi\Omega^2/2A\omega}-1}}, \tag{42}$$

which can easily be solved numerically. It is possible to derive a simple approximate solution in the adiabatic regime ($\Omega^2\gg A\omega$). Then the right-hand side of Eq. (42) is approximately zero, and also $\phi\approx 0$, $\phi_{\rm ad}\approx(\pi/4\omega)[z-A^2/4z+\cdots]$ with $z=\sqrt{\Omega^2+A^2}$. After some simple algebra we find

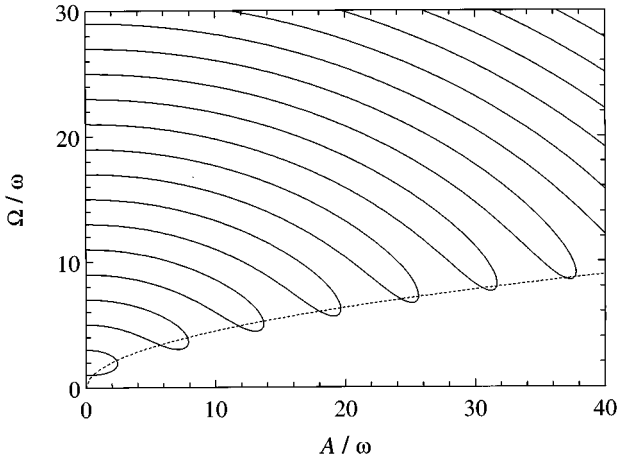

FIG. 7. The exact curves in the parameter plane $(\Omega/\omega, A/\omega)$ on which $p=\frac{1}{2}$, obtained by numerical integration of Eqs. (1). We have found that they practically coincide with those derived from Eq. (42) (not shown on the figure). The dashed curve $[(\Omega/\omega)^2=2A/\omega]$ gives an idea of the boundary between the regions where the evolution is adiabatic (above) and where the evolution is nonadiabatic (below).

$$\sqrt{(\Omega/\omega)^2+(A/\omega)^2}\approx\frac{1}{2}[n+\sqrt{n^2+A^2/\omega^2}]$$

$$(n=1,3,5,\ldots;\Omega^2\gg A\omega). \quad (43)$$

This equation defines a family of infinite number of curves labeled by the odd index n. In Fig. 7, we present the exact curves in the parameter plane $(\Omega/\omega, A/\omega)$ on which $p=\frac{1}{2}$, obtained by numerical integration of Eqs. (1). We have found that they practically coincide with those derived from Eq. (42) (not shown on the figure). We have also checked that in the adiabatic regime (roughly above the dashed curve) the $p=\frac{1}{2}$ curves are well approximated by the curves defined in Eq. (43).

We must stress that the condition $p=\frac{1}{2}$ is necessary and sufficient for population swapping to occur. In fact, cases of approximate population swapping have been shown in Figs. 1 and 2 of Ref. [14] in which the ratio A/ω has been chosen to satisfy the condition $J_0(A/\omega)=0$. The present analysis shows that the condition $J_0(A/\omega)=0$ is only important for small coupling (Sec. II B). For instance, for the parameters in Fig. 2 of Ref. [14], $A/\omega=j_{0,10}=30.6346\ldots$ and $\Omega/\omega=8$, we have $p\approx0.51915$, which indeed is very close to $p=\frac{1}{2}$. In Fig. 8(a), the population evolution is shown for $A/\omega=j_{0,10}=30.6346\ldots$ and $\Omega/\omega=8$ (the same parameters from Fig. 2 of Ref. [14]), with $\varphi=0$. Almost complete population swapping is realized. In Fig. 8(b), we show the population evolution for $A/\omega=j_{0,10}=30.6346\ldots$ [the condition $J_0(A/\omega)=0$ is again fulfilled] but with $\Omega/\omega=4.81398$ (then $p\approx0.192641, P\approx0.5$). A rather different behavior is observed, the excited-state population being almost zero for every fourth half period and around $\frac{2}{3}$ for the other three half periods. This specific case is further discussed in Sec. V C. Hence, Fig. 8(b) shows that the condition $J_0(A/\omega)=0$ does not necessarily ensure population swapping. In Fig. 8(c), the population evolution is shown for $A/\omega=j_{1,9}=29.0468\ldots$ [the ninth zero of $J_1(A/\omega)$ where $J_0(A/\omega)$ has an extremum rather than a zero] and $\Omega/\omega=8.96149$ (then $p\approx0.5$). Figure 8(c) exhibits almost perfect population swapping despite the fact that the condition $J_0(A/\omega)=0$ is significantly violated. Thus, Fig. 8 demonstrates clearly that it is the condition

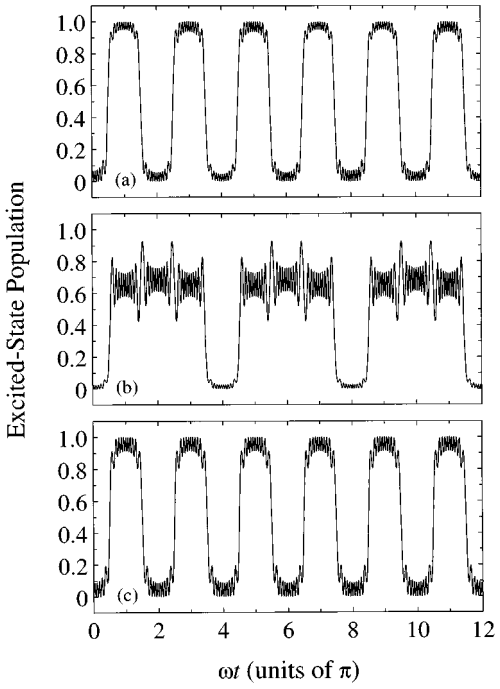

FIG. 8. The excited-state population evolution for $\varphi=0$ and (a) $A/\omega=j_{0,10}=30.6346\ldots$ [the tenth zero of $J_0(A/\omega)$] and $\Omega/\omega=8$; (b) $A/\omega=j_{0,10}=30.6346\ldots$ and $\Omega/\omega=4.81398$ (where $p\approx0.192641, P\approx0.5$); (c) $A/\omega=j_{1,9}=29.0468\ldots$ [the ninth zero of $J_1(A/\omega)$] and $\Omega/\omega=8.96149$ (where $p\approx0.5$).

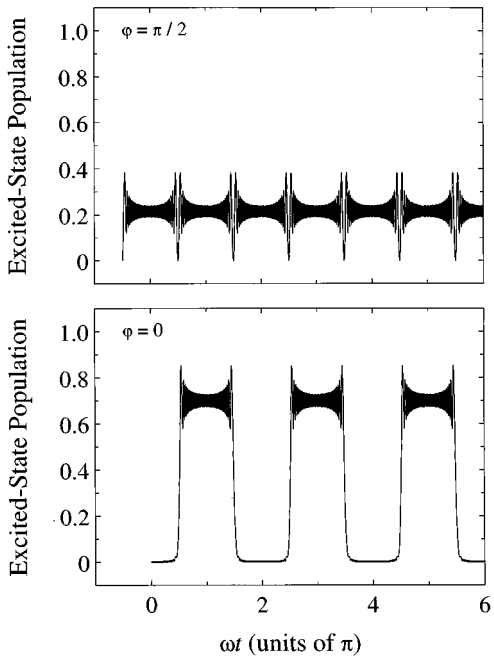

FIG. 9. Cases of incomplete population swapping (for $\varphi=0$) and superpositional trapping (for $\varphi=\pi/2$). The parameters are $\Omega/\omega=12, A/\omega=202.1261$ (there $P\approx0, p\approx0.23901$).

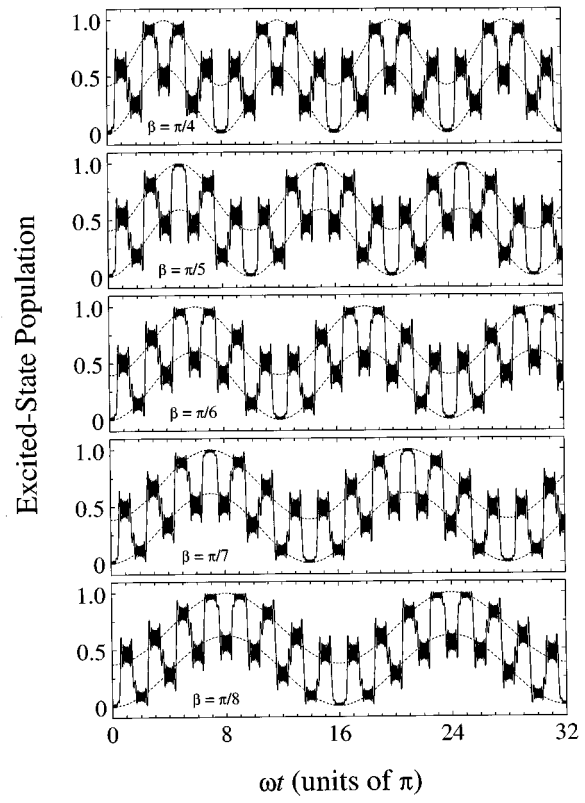

FIG. 10. Examples of completely periodic evolution for $A/\omega=24$ and several values of Ω/ω: 3.99018, 3.77660, 3.62346, 3.50735, and 3.41581, chosen in such a way that $\beta\approx\pi/4,\pi/5,\pi/6,\pi/7$, and $\pi/8$, respectively. The dashed curves show the global structures (23) and (24). As Eq. (21) suggests and the figure demonstrates, for $\beta=\pi/s$ with s odd, the excited-state population equals unity at the sth, $(3s)$th, $(5s)$th, etc., antinodes and the system is completely inverted there.

$p=\frac{1}{2}$ that is responsible for population swapping rather than $J_0(A/\omega)=0$.

Finally, we note that as seen from Eq. (38), in the adiabatic regime $[(\Omega/\omega)^2\gg A/\omega]$ p tends to $\frac{1}{2}$ for $A\gg\Omega$. In fact, this property is a consequence of the asymmetry of the two-level problem in the interval $[0,\pi/2]$ [19] . The appearance of population swapping in this case confirms from another viewpoint the conclusion deduced in Sec. II C from the adiabatic solution and illustrated in Fig. 3.

B. Incomplete population swapping and superpositional trapping ($P=0$)

Another interesting case arises when $P=0$. Then $\beta=0$ and according to Eqs. (20), (21), (26), and (27), we have $P_{\varphi=0}(2N\pi)=0$, $P_{\varphi=0}[(2N+1)\pi]=4p(1-p)$, and $P_{\varphi=\pi/2}(N\pi)=p$. Hence, for cosine modulation the excited-state population jumps successively from 0 to $4p(1-p)$ and vice versa. Since $4p(1-p)<1$ for $p\neq\frac{1}{2}$, the *population swapping is incomplete*. For sine modulation the excited-state population stays around p; i.e., we encounter a case of approximate *superpositional trapping*. Unlike the case of population trapping considered in Sec. II B, where the population is trapped in a *single* diabatic state, here the population is trapped in a coherent *superposition* of states, namely, in the state $\sqrt{1-p}|1\rangle+\sqrt{p}|2\rangle$, up to an unimportant common phase factor. Cases of incomplete population swapping (for $\varphi=0$) and superpositional trapping (for $\varphi=\pi/2$) are shown in Fig. 9. According to our analytic approximation (33), the condition $P=0$ is met when $\sin(\phi+2\phi_a)\approx 0$. We have verified that this is in very good agreement with the exact numerical calculations. Finally, when both $P=0$ and $p=\frac{1}{2}$, the population swapping is complete, as it should be for $p=\frac{1}{2}$ according to Sec. V A.

C. Completely periodic evolution

When $\beta\equiv\arccos(1-2P)$ is a rational multiple of π, $\beta=r\pi/s$ (r,s integers), the excited-state population $P_{\varphi=0}(2N\pi)$ [Eq. (20)] vanishes exactly at every $(2s)$th antinode. Thus, the initial conditions are restored, which implies that the population evolution is exactly the same in the intervals $[0,2s\pi],[2s\pi,4s\pi],\ldots$. The population swapping regime in subsection V B (when $P=0$ and hence $\beta=0$) represents the simplest example of such evolution. In Fig. 10, we show examples of completely periodic evolution for $A/\omega=24$ and several values of Ω/ω, chosen in such a way that $\beta\approx\pi/4,\pi/5,\pi/6,\pi/7$, and $\pi/8$, respectively. As Eq. (21) suggests and the figure demonstrates, for $\beta=\pi/s$

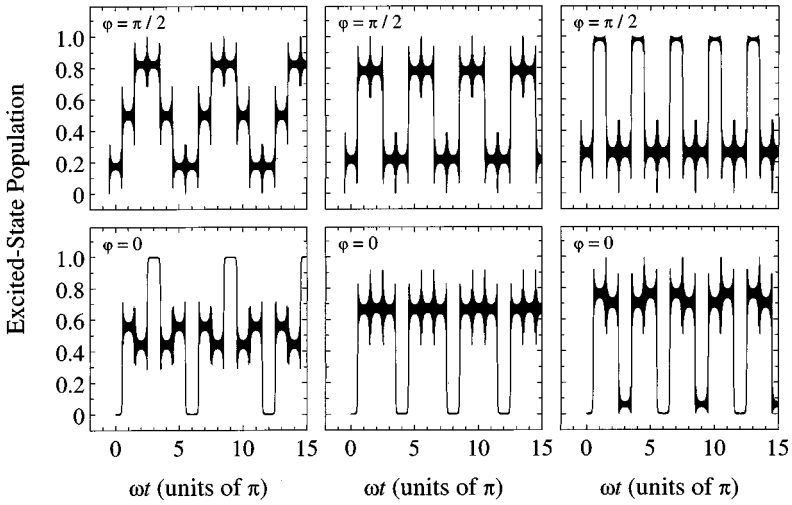

FIG. 11. Examples of completely periodic evolution with small periods when $\beta\approx\pi/3$ ($P\approx\frac{1}{4}$), $\beta\approx\pi/2$ ($P\approx\frac{1}{2}$), and $\beta\approx 2\pi/3$ ($P\approx\frac{3}{4}$). The ratio $A/\omega=200$ everywhere and $\Omega/\omega=10.47732$ (the two figures on the left-hand side), $\Omega/\omega=12.02304$ (the two figures in the middle), and $\Omega/\omega=13.66601$ (the two figures on the right-hand side). These cases more closely resemble the regime of population swapping.

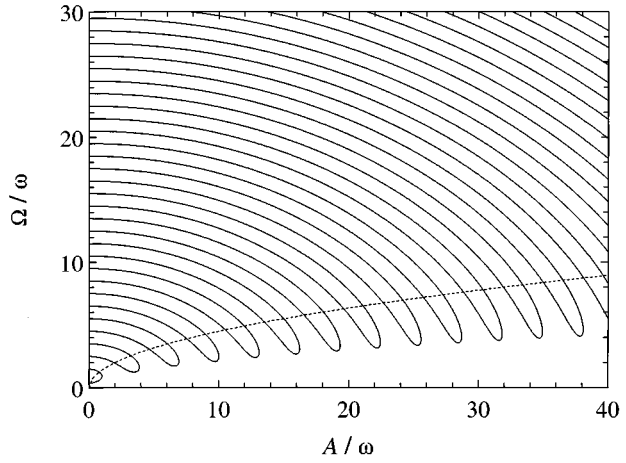

FIG. 12. The exact curves in the parameter plane $(\Omega/\omega, A/\omega)$ on which $P=\frac{1}{2}$, found by numerical integration of Eqs. (1). The dashed curve $[(\Omega/\omega)^2=2A/\omega]$ gives an idea of the boundary between the regions where the evolution is adiabatic (above) and where the evolution is nonadiabatic (below).

with s odd, the excited-state population equals unity at the sth, $(3s)$th, $(5s)$th, etc. antinodes and the system is completely inverted there.

In Fig. 11, we show examples of completely periodic evolution for smaller periods when $\beta\approx\pi/3$ $(P\approx\frac{1}{4})$, $\beta\approx\pi/2$ $(P\approx\frac{1}{2})$, and $\beta\approx 2\pi/3$ $(P\approx\frac{3}{4})$. These cases more closely resemble the regime of population swapping. We encounter some curious cases of population evolution: ''twice down, once middle, twice up'' (top left figure), ''once down, twice middle, once up'' (bottom left figure), ''twice down, twice up'' (top middle figure), ''once down, three times up'' (bottom middle figure), ''twice down, once up'' (top right figure), ''once down, twice up'' (bottom right figure). We particularly emphasize the bottom figure in the middle $(\varphi=0, P=\frac{1}{2})$, which shows superpositional trapping around the value of $\frac{2}{3}$ for three half periods and trapping in the ground state for the fourth half period, a case earlier seen in Fig. 8(b). In Fig. 12, we show the curves in the parameter plane $(\Omega/\omega, A/\omega)$ on which $P=\frac{1}{2}$. They resemble those for $p=\frac{1}{2}$ in Fig. 7, but are twice as dense as follows from Eqs. (32) and (33). One can derive an approximation to the $P=\frac{1}{2}$ curves similar to that [Eq. (43)] for the $p=\frac{1}{2}$ curves.

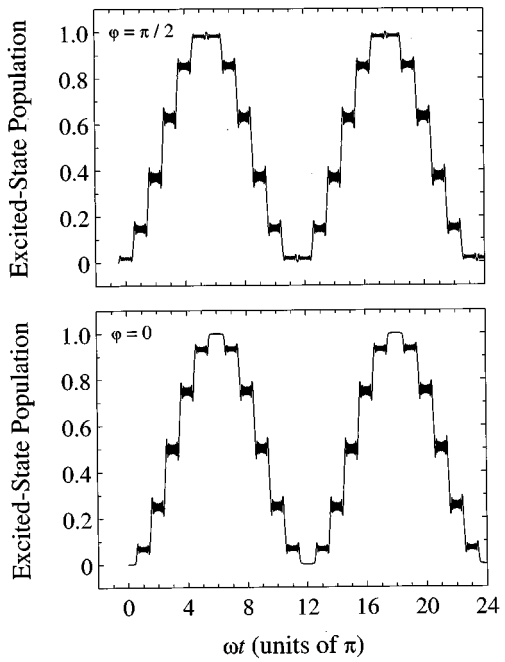

FIG. 13. The excited-state population evolution for $\varphi=0$ and $\varphi=\pi/2$ in the case of $A/\omega=32$ and $\Omega/\omega=1.2007$. The condition $P=4p(1-p)$ is fulfilled almost exactly for these parameters and stepwise evolution is realized not only for sine modulation $(\varphi=\pi/2)$ but also for cosine modulation $(\varphi=0)$.

D. Stepwise evolution

As we pointed out in Sec. III, the implication from the existence of only one global structure for sine modulation is that if the jumps at the crossings are small enough, the global excitation history is a *stepwise* trajectory. For cosine modulation, the global evolution depends on the shift (25) between the two global structures. If this shift is large enough, then the evolution involves alternative *upward and downward jumps* as in Figs. 4 and 10. It is readily seen that for $P=4p(1-p)$ the shift (25) vanishes and the evolution should be a stepwise trajectory (if the ''jumps'' at the crossings are small enough) as for sine modulation. Such an example is shown in Fig. 13.

VI. CONCLUSIONS

We have presented an analytic study of the population dynamics of a nondissipative two-state system interacting with an external field and subjected to periodic level crossings. We have used a new evolution matrix approach to calculate the excited-state population at the crossings (the nodes) and at the antinodes. The results depend on only two parameters: the transition probability p for a quarter period from a crossing to an antinode and the transition probability P for a half period between two successive crossings. We have found that the values of the excited-state population at the antinodes form global (gross) structures. The results are generally valid for any modulation with a period of 2π such that the detuning is symmetric in the interval $[0,\pi]$ and antisymmetric in $[0,2\pi]$. We have been mainly concerned with the sinusoidal modulation (2), which is the most natural one. We have concluded that the global structures and the population dynamics as a whole are very sensitive to the initial phase φ of the frequency-modulated field. Particular attention has been paid to the cases $\varphi=0$ (cosine modulation) and $\varphi=\pi/2$ (sine modulation), which lead to the most extreme differences in the population dynamics. We have calculated the parameters p and P by using two approaches based on the original LZ model and the finite LZ model, which turn out to lead to the same results, Eqs. (32) and (33). The notion of the global structures and the relevant parametrization in terms of p and P have allowed us to find various distinctive cases of population dynamics, such as population swapping, completely periodic evolution, superpositional trapping, and stepwise evolution. Finally, we note that physical systems exist where it should be possible to observe these phenomena. It has already been suggested that, for example, the Yb

atom could be used in conjunction with frequency modulated light [14,20], and it may also prove possible to manipulate the discrete optical levels in a resonator to show the same phenomena [21].

ACKNOWLEDGMENTS

The authors acknowledge the useful discussions of some of the results in this paper with Professor P. L. Knight and Dr. K.-A. Suominen. This work was supported in part by the Royal Society, the UK Engineering and Physical Sciences Research Council, the European Union, and the Research Institute for Theoretical Physics in Helsinki.

APPENDIX A: ADIABATIC-FOLLOWING SOLUTION

The transformation

$$\mathbf{c}(t)=\begin{bmatrix} e^{-iD(t)/2} & 0 \\ 0 & e^{iD(t)/2} \end{bmatrix}\mathbf{b}(t),$$

where $D(t)=\int_0^t\Delta(t')dt'$, casts Eqs. (1) into their Schrödinger representation

$$i\frac{d}{dt}\mathbf{b}(t)=\frac{1}{2}\begin{bmatrix} -\Delta(t) & \Omega \\ \Omega & \Delta(t) \end{bmatrix}\mathbf{b}(t). \tag{A1}$$

The time-dependent rotation $\mathbf{b}(t)=\mathbf{R}(\frac{1}{2}\vartheta(\omega t))\mathbf{a}(t)$ with

$$\mathbf{R}(\gamma)=\begin{bmatrix} \cos\gamma & \sin\gamma \\ -\sin\gamma & \cos\gamma \end{bmatrix}$$

transforms Eqs. (A1) into the adiabatic representation

$$i\frac{d}{dt}\mathbf{a}=\frac{1}{2}\begin{bmatrix} -\Omega_0 & -i\dot{\vartheta} \\ i\dot{\vartheta} & \Omega_0 \end{bmatrix}\mathbf{a}, \tag{A2}$$

where ϑ and Ω_0 are defined by Eqs. (8) and (9). The condition for adiabatic evolution is $|\dot{\vartheta}|\ll\Omega_0$ and if it is fulfilled then the evolution matrix in the adiabatic basis is nearly diagonal. The adiabatic-following solution is $\mathbf{a}(t)=\mathbf{U}^a_{\rm ad}(\omega t,\omega t_0)\mathbf{a}(t_0)$ with

$$\mathbf{U}^a_{\rm ad}(\omega t,\omega t_0)=\begin{bmatrix} e^{i\phi_{\rm ad}(\omega t_0,\omega t)} & 0 \\ 0 & e^{-i\phi_{\rm ad}(\omega t_0,\omega t)} \end{bmatrix}, \tag{A3}$$

where $\phi_{\rm ad}(\omega t_0,\omega t)$ is the adiabatic phase defined by Eq. (12) and acquired between times t_0 and t. The adiabatic solution in the actual (bare, diabatic) basis is $\mathbf{b}(t)=\mathbf{U}^b_{\rm ad}(\omega t,\omega t_0)\mathbf{b}(t_0)$, where the evolution matrix is given by

$$\mathbf{U}^b_{\rm ad}(\omega t,\omega t_0)=\mathbf{R}(\vartheta(\omega t)/2)\mathbf{U}^a_{\rm ad}(\omega t,\omega t_0)\mathbf{R}^T[\vartheta(\omega t_0)/2]$$

$$=\begin{bmatrix} u & v \\ -v^* & u^* \end{bmatrix}, \tag{A4}$$

$$u=\cos\phi_{\rm ad}\cos\frac{\vartheta-\vartheta_0}{2}+i\sin\phi_{\rm ad}\cos\frac{\vartheta+\vartheta_0}{2}, \tag{A5}$$

$$v=\cos\phi_{\rm ad}\sin\frac{\vartheta-\vartheta_0}{2}-i\sin\phi_{\rm ad}\sin\frac{\vartheta+\vartheta_0}{2}, \tag{A6}$$

with the short-hand notation $\vartheta\equiv\vartheta(\omega t)$, $\vartheta_0\equiv\vartheta(\omega t_0)$, and $\phi_{\rm ad}\equiv\phi_{\rm ad}(\omega t_0,\omega t)$. The excited-state population is $P_{\rm ad}=|v|^2$ and is given explicitly by Eq. (11).

APPENDIX B: GLOBAL STRUCTURES

We wish to calculate the evolution matrices for Eqs. (1) in the intervals $[0,2N\pi]$, $[0,(2N+1)\pi]$, $[-\pi/2,2N\pi]$, and $[-\pi/2,(2N+1)\pi]$. Since the elements of any 2×2 unitary matrix $\mathbf{U}$ with $\det\mathbf{U}=1$ obey the relations $U_{11}=U_{22}^*$ and $U_{12}=-U_{21}^*$, we will only give two elements of each matrix below. In addition to the relations (14)–(17), we will use the following identity valid for any unitary matrix [22]

$$\begin{bmatrix} U_{11} & U_{12} \\ -U_{12}^* & U_{11}^* \end{bmatrix}^N$$

$$=\begin{bmatrix} \cos N\beta+i\ \mathrm{Im}U_{11}\dfrac{\sin N\beta}{\sin\beta} & U_{12}\dfrac{\sin N\beta}{\sin\beta} \\ -U_{12}^*\dfrac{\sin N\beta}{\sin\beta} & \cos N\beta-i\ \mathrm{Im}U_{11}\dfrac{\sin N\beta}{\sin\beta} \end{bmatrix}, \tag{B1}$$

where $\cos\beta=\mathrm{Re}U_{11}$. We will need the evolution matrices for the intervals $[0,2\pi]$ and $[\pi,3\pi]$. According to Eqs. (14)–(17) they are given by

$$\mathbf{U}(2\pi,0)=\mathbf{U}^T\sigma_3\mathbf{U}^*\mathbf{U}^\dagger\sigma_3\mathbf{U},$$

$$\mathbf{U}(3\pi,\pi)=\sigma_3\mathbf{U}^\dagger\sigma_3\mathbf{U}\mathbf{U}^T\sigma_3\mathbf{U}^*\sigma_3=\sigma_3[\mathbf{U}(2\pi,0)]^*\sigma_3.$$

In terms of the parameters of $\mathbf{U}$ defined by Eq. (13) and $P=4p(1-p)\sin^2\eta$, the matrix elements of $\mathbf{U}(2\pi,0)$ and $\mathbf{U}(3\pi,\pi)$ read

$$U_{11}(2\pi,0)=U_{11}^*(3\pi,\pi)=1-2P+4ip(1-p)\sin2\eta, \tag{B2}$$

$$U_{12}(2\pi,0)=U_{12}(3\pi,\pi)=-2i(1-2p)\sqrt{P}. \tag{B3}$$

Due to Eq. (17), for the interval $[0,2N\pi]$ we have $\mathbf{U}(2N\pi,0)=[\mathbf{U}(2\pi,0)]^N$ and by using Eqs. (B1), (B2), and (B3) we obtain

$$U_{11}(2N\pi,0)=\cos N\beta+4ip(1-p)\sin2\eta\frac{\sin N\beta}{\sin\beta}, \tag{B4}$$

$$U_{12}(2N\pi,0)=-2i(1-2p)\sqrt{P}\frac{\sin N\beta}{\sin\beta}, \tag{B5}$$

where $\cos\beta = 1-2P$. Likewise, for the interval $[0,(2N+1)\pi]$ we use that $\mathbf{U}[(2N+1)\pi,0] = \mathbf{U}[(2N+1)\pi,\pi]\mathbf{U}(\pi,0) = [\mathbf{U}(3\pi,\pi)]^N \sigma_3 \mathbf{U}^\dagger \sigma_3 \mathbf{U}$ and we find

$$U_{11}[(2N+1)\pi,0] = \frac{1-2p}{\sqrt{1-P}} \cos\left(N+\frac{1}{2}\right)\beta, \tag{B6}$$

$$U_{12}[(2N+1)\pi,0] = \frac{\sqrt{4p(1-p)-P}}{\sqrt{1-P}} \cos\left(N+\frac{1}{2}\right)\beta - i \sin\left(N+\frac{1}{2}\right)\beta. \tag{B7}$$

By using $\mathbf{U}(2N\pi,-\pi/2) = \mathbf{U}(2N\pi,0)\mathbf{U}^T$ and $\mathbf{U}[(2N+1)\pi,-\pi/2] = \mathbf{U}[(2N+1)\pi,0]\mathbf{U}^T$, we further obtain with the help of Eqs. (B4)–(B7)

$$U_{11}[2N\pi,-\pi/2] = \frac{e^{i(\zeta-\eta)/2}}{2\sqrt{p(1-P)}} \left\{ \sqrt{4p(1-p)-P}\, \cos\left(N+\frac{1}{2}\right)\beta + i\left[\sqrt{P}\, \cos\left(N+\frac{1}{2}\right)\beta + 2p\, \sin N\beta \right] \right\}, \tag{B8}$$

$$U_{12}[2N\pi,-\pi/2] = -\frac{e^{i(\eta-\zeta)/2}}{2\sqrt{p(1-P)}} \left\{ \left[\sqrt{P}\, \sin N\beta + 2p\, \cos\left(N+\frac{1}{2}\right)\beta \right] + i\sqrt{4p(1-p)-P}\, \sin N\beta \right\}, \tag{B9}$$

$$U_{11}[(2N+1)\pi,-\pi/2] = \frac{e^{i(\zeta-\eta)/2}}{2\sqrt{p(1-P)}} \left\{ \sqrt{4p(1-p)-P}\, \cos\left(N+\frac{1}{2}\right)\beta + i\left[\sqrt{P}\, \cos\left(N+\frac{1}{2}\right)\beta - 2p\, \sin(N+1)\beta \right] \right\}, \tag{B10}$$

$$U_{12}[(2N+1)\pi,-\pi/2] = \frac{e^{i(\eta-\zeta)/2}}{2\sqrt{p(1-P)}} \left\{ \left[2p\, \cos\left(N+\frac{1}{2}\right)\beta - \sqrt{P}\, \sin(N+1)\beta \right] - i\sqrt{4p(1-p)-P}\, \sin(N+1)\beta \right\}. \tag{B11}$$

APPENDIX C: CALCULATION OF *p* AND *P* BY USING THE FINITE LANDAU-ZENER MODEL

For the sake of convenience, we choose to derive p and P by working with a detuning $\Delta(t) = A \sin\omega t$ and with the two-level equations in their Schrödinger representation (A1) in order to use directly the recent results for the finite Landau-Zener model [15], which assumes a linear crossing at $t=0$ with a positive slope. It can easily be shown that the evolution matrix in the time interval $[0,\pi/2]$ is $\mathbf{U}^T\mathbf{M}$, where $\mathbf{U}$ is the quarter-period evolution matrix for cosine modulation (13) and

$$\mathbf{M} = \begin{bmatrix} e^{iA/2\omega} & 0 \\ 0 & e^{-iA/2\omega} \end{bmatrix}. \tag{C1}$$

Thus, the transition probability is exactly $|(\mathbf{U}^T\mathbf{M})_{12}|^2 = |U_{12}|^2 \equiv p$. Furthermore, for the time interval $[0,\pi]$ the evolution matrix is $\mathbf{M}^*\mathbf{U}\mathbf{U}^T\mathbf{M}$ and hence, the transition probability is given by $|(\mathbf{M}^*\mathbf{U}\mathbf{U}^\mathbf{T}\mathbf{M})_{12}|^2 = |(\mathbf{U}\mathbf{U}^T)_{12}|^2 \equiv P$.

We begin with the calculation of p. We separate the time evolution in $[0,\pi/2]$ into two parts: $[0,\omega T]$ and $[\omega T,\pi/2]$, where T is a free matching parameter ($0 < \omega T < \pi/2$). In the interval $[0,\omega T]$, i.e., near the crossing where $\Delta(t) = A \sin\omega t$ is almost linear, we calculate the evolution matrix by using the half-crossing finite LZ model [15] in order to account for nonadiabatic transitions. In the interval $[\omega T,\pi/2]$ we assume that the evolution is adiabatic and we use the adiabatic-following solution (Appendix A). The exact finite LZ evolution matrix in the Schrödinger representation (A1) is given by [15]

$$\mathbf{U}^b_{\mathrm{FLZ}}(\tau,0) = \begin{bmatrix} x & y \\ -y^* & x^* \end{bmatrix}, \tag{C2}$$

$$x = \frac{2^{-i\alpha^2/4}}{2\sqrt{\pi}} \Gamma\left(\frac{1}{2} - i\frac{\alpha^2}{4}\right) [D_{i\alpha^2/2}(\tau\sqrt{2}e^{-i\pi/4}) + D_{i\alpha^2/2}(\tau\sqrt{2}e^{3i\pi/4})],$$

$$y = \frac{2^{-i\alpha^2/4}}{\alpha\sqrt{\pi}} e^{i\pi/4} \Gamma\left(1 - i\frac{\alpha^2}{4}\right) [-D_{i\alpha^2/2}(\tau\sqrt{2}e^{-i\pi/4}) + D_{i\alpha^2/2}(\tau\sqrt{2}e^{3i\pi/4})],$$

where $\tau = T\sqrt{A\omega/2}$ and $\alpha = \Omega/\sqrt{2A\omega}$ while $D_\nu(z)$ is the parabolic cylinder function [23]. These matrix elements are well approximated by using the so-called strong-coupling asymptotics of $D_\nu(z)$ [15]; the final expressions are

$$x \sim e^{i\mu_1}[\sin(\vartheta_{\mathrm{LZ}}/2)\, \sin(\chi/2) e^{-i\xi} + \cos(\vartheta_{\mathrm{LZ}}/2)\, \cos(\chi/2)], \tag{C3}$$

$$y \sim e^{i\mu_2}[\sin(\vartheta_{\mathrm{LZ}}/2)\, \cos(\chi/2) e^{-i\xi} - \cos(\vartheta_{\mathrm{LZ}}/2)\, \sin(\chi/2)], \tag{C4}$$

with

$$\xi=\phi+2\phi_{\rm LZ}, \tag{C5}$$

where ϕ is the Landau-Zener phase (36), $\phi_{\rm LZ}$ is the adiabatic phase in the finite LZ model,

$$\phi_{\rm LZ}=\int_0^{\tau}\sqrt{\alpha^2+\tau'^2}\,d\tau'$$

$$=\frac{\tau}{2}\sqrt{\tau^2+\alpha^2}+\frac{\alpha^2}{2}\ln\left[\frac{1}{\alpha}(\tau+\sqrt{\tau^2+\alpha^2})\right], \tag{C6}$$

and

$$\mu_1=\phi_{\rm LZ}-\frac{\alpha^2}{4}+\frac{\alpha^2}{2}\ln\frac{\alpha}{2}+\arg\Gamma\left(\frac{1}{2}-i\frac{\alpha^2}{4}\right),$$

$$\mu_2=\phi_{\rm LZ}-\frac{\alpha^2}{4}+\frac{\alpha^2}{2}\ln\frac{\alpha}{2}+\arg\Gamma\left(1-i\frac{\alpha^2}{4}\right)+\frac{\pi}{4},$$

$$\tan\vartheta_{\rm LZ}=\frac{\alpha}{\tau}=\frac{\Omega}{\omega AT}\quad(0\leqslant\vartheta_{\rm LZ}\leqslant\pi/2),$$

$$\cos\chi=e^{-\pi\alpha^2/2}\quad(0\leqslant\chi\leqslant\pi/2).$$

For the interval $[\omega T,\pi/2]$ we use the adiabatic-following solution (Appendix A). By multiplying the adiabatic evolution matrix (A4)–(A6) for the interval $[\omega T,\pi/2]$ and the finite LZ matrix (C2)–(C4) for the interval $[0,\omega T]$ we find

$$\mathbf{U}^T\mathbf{M}\approx\mathbf{U}^b_{\rm ad}(\pi/2,\omega T)\mathbf{U}^b_{\rm FLZ}(\omega T,0)$$

$$\approx\begin{bmatrix} ux-vy^* & uy+vx^* \\ -u^*y^*-v^*x & u^*x^*-v^*y\end{bmatrix} \tag{C7}$$

and, hence,

$$p\approx|uy+vx^*|^2$$

$$\approx\tfrac{1}{2}[1-\cos\chi\,\cos\Theta-\sin\chi\,\sin\Theta\,\cos(\phi+2\phi_{\rm ad})], \tag{C8}$$

where $\Theta\equiv\vartheta(\pi/2)=\arctan(\Omega/A)$. In the derivation of Eq. (C8), we have assumed that $\vartheta_{\rm LZ}\approx\vartheta$ and $\phi_{\rm LZ}\approx\phi_{\rm ad}$ at $t=T$. These assumptions simplify the result, eliminate the dependence on the matching point T, and compensate to some extent the inaccuracy introduced by the difference between the time dependence of the actual detuning $\Delta(t)=A\sin\omega t$ and the linear LZ detuning.

We now turn to the calculation of $P\equiv|(\mathbf{U}\mathbf{U}^T)_{12}|^2$. Since for the time interval $[0,\pi]$ the evolution matrix in the Schrödinger representation (A1) is $\mathbf{M}^*\mathbf{U}\mathbf{U}^{\mathbf{T}}\mathbf{M}=(\mathbf{M}^*)^2(\mathbf{U}^T\mathbf{M})^T(\mathbf{U}^T\mathbf{M})$, we find from Eq. (C7) that

$$P\approx\sin^2\chi\,\sin^2(\phi+2\phi_{\rm ad}), \tag{C9}$$

with the same assumptions as in the derivation of p.

APPENDIX D: CALCULATION OF p AND P BY USING THE ORIGINAL LANDAU-ZENER MODEL

We have also determined p and P by using the original Landau-Zener model, which assumes a constant coupling lasting from $t\to-\infty$ to $t\to+\infty$ and a linear detuning passing through the resonance at $t=0$. This cannot be done directly for a quarter period (for p) and a half period (for P) as in Appendix C because there is no complete level crossing but only half crossings in these time intervals. Instead, one can determine p and P indirectly. The parameter p can be found by deriving the transition probability from a given antinode to the next antinode, which, according to Eq. (21) with $N=0$, is equal to $4p(1-p)$; we choose to do this in the interval $[-\pi/2,\pi/2]$ with sine modulation, $\Delta(t)=A\sin\omega t$. Then, the parameter P can be found from the transition probability from a given lower (or upper) antinode to the next lower (or upper) antinode, which is equal to $4P(1-2p)^2$, according to Eq. (20) with $N=1$; we choose for this the interval $[-\pi/2,3\pi/2]$ with sine modulation, $\Delta(t)=A\sin\omega t$, again. We assume that the evolution is purely adiabatic throughout except at the crossings where instantaneous nonadiabatic LZ transitions take place. It is convenient to work in the adiabatic interaction representation

$$\frac{d}{dt}\mathbf{d}(t)$$

$$=\begin{bmatrix} 0 & -\frac{1}{2}\dot{\vartheta}(\omega t)e^{-2i\phi_{\rm ad}(0,\omega t)} \\ \frac{1}{2}\dot{\vartheta}(\omega t)e^{2i\phi_{\rm ad}(0,\omega t)} & 0\end{bmatrix}\mathbf{d}(t) \tag{D1}$$

obtained from the adiabatic Schrödinger representation (A2) with the transformation

$$\mathbf{a}(t)=\mathbf{U}^a_{\rm ad}(\omega t,0)\mathbf{d}(t),$$

where $\mathbf{U}^a_{ad}(\omega t,0)$ is defined by Eq. (A3). It is this representation (D1) where the evolution-matrix phases in the original LZ model are defined (in any other representation they diverge). Furthermore, in the adiabatic limit the probability amplitudes $\mathbf{d}(t)$ do not change and thus the adiabatic evolution matrix is the unity matrix.

In this model, the evolution matrix in the interval $[-\pi/2,\pi/2]$ is given by

$$\mathbf{U}^d(\pi/2,-\pi/2)\approx\mathbf{U}^d_{\rm LZ}=\begin{bmatrix}\sqrt{1-p_{\rm LZ}}e^{i\phi} & \sqrt{p_{\rm LZ}} \\ -\sqrt{p_{\rm LZ}} & \sqrt{1-p_{\rm LZ}}e^{-i\phi}\end{bmatrix},$$

with $p_{\rm LZ}=e^{-\pi\alpha^2}=\cos^2\chi$, $\alpha=\Omega/\sqrt{2A\omega}$ and ϕ is given by Eq. (36). The evolution matrix for the actual (bare) amplitudes $\mathbf{b}(t)$ is

$$\mathbf{U}^b(\pi/2,-\pi/2)\approx\mathbf{R}(\vartheta(\pi/2)/2)\mathbf{U}^a_{\rm ad}(\pi/2,0)\mathbf{U}^d_{\rm LZ}$$

$$\times(\mathbf{U}^a_{\rm ad}(0,-\pi/2))^*\mathbf{R}^T(\vartheta(-\pi/2)/2).$$

From here we find

$$4p(1-p)=|U^b_{12}(\pi/2,-\pi/2)|^2$$

$$\approx1-[\cos\chi\,\cos\Theta+\sin\chi\,\sin\Theta\,\cos(\phi+2\phi_{\rm ad})]^2,$$

where $\Theta \equiv \vartheta(\pi/2)$ and $\phi_{\rm ad} \equiv \phi_{\rm ad}(0,\pi/2)$, which leads to the same result (C8) as from using the finite LZ model.

To find P we need the evolution matrix for the time interval $[-\pi/2,3\pi/2]$; it is

$$\mathbf{U}^b(3\pi/2,-\pi/2) = \mathbf{M}(\mathbf{U}^b(\pi/2,-\pi/2))^T \mathbf{U}^b(\pi/2,-\pi/2)\mathbf{M}^*.$$

The transition probability in this interval is

$$4P(1-2p)^2 = |U_{12}^b(3\pi/2,-\pi/2)|^2 \approx 4(1-2p)^2 \sin^2\chi \sin^2(\phi+2\phi_{\rm ad})$$

and we obtain again the same result (C9) as from the finite LZ model in Appendix C.

[1] L.D. Landau, Phys. Z. Sowjetunion **2**, 46 (1932); C. Zener, Proc. R. Soc. London Ser. A **137**, 696 (1932).

[2] N. Rosen and C. Zener, Phys. Rev. **40**, 502 (1932).

[3] I.I. Rabi, Phys. Rev. **51**, 652 (1937).

[4] B.W. Shore, *The Theory of Coherent Atomic Excitation* (Wiley, New York, 1990).

[5] E.E. Nikitin and S.Ya. Umanskii, *Theory of Slow Atomic Collisions* (Springer-Verlag, Berlin, 1984).

[6] J.M. Ziman, *Principles of the Theory of Solids* (Cambridge University Press, London, 1972).

[7] M. Baer, in *Theory of Chemical Reaction Dynamics*, edited by M. Baer (CRC, Boca Raton, FL, 1985), Vol. 2, p. 219; J.C. Tully, in *Modern Theoretical Chemistry, Part B*, edited by W.H. Miller (Plenum, New York, 1976), Chap. 5; J. Ulstrup, *Charge Transfer Processes in Condensed Media* (Springer-Verlag, Berlin, 1979).

[8] R.A. Marcus and N. Sutin, Biochim. Biophys. Acta **811**, 265 (1985); *Tunneling in Biological Systems*, edited by B. Chance, D.C. DeVault, H. Frauenfelder, R.A. Marcus, J.R. Schrieffer, and N. Sutin (Academic, New York, 1979); D. DeVault, *Quantum Mechanical Tunneling in Biological Systems* (Cambridge University Press, London, 1984).

[9] F. Grossmann, T. Dittrich, P. Jung, and P. Hänggi, Phys. Rev. Lett. **67**, 516 (1991); F. Grossmann, P. Jung, T. Dittrich, and P. Hänggi, Z. Phys. B **84**, 315 (1991); F. Grossmann and P. Hänggi, Europhys. Lett. **18**, 571 (1992).

[10] J.-M. Lopez-Castillo, A. Filali-Mouhim, and J.-P. Jay-Gerin, J. Chem. Phys. **97**, 1905 (1992); R.I. Cukier, M. Morillo, and J.M. Casado, Phys. Rev. B **45**, 1213 (1992); J.M. Gomez Llorente and J. Plata, Phys. Rev. A **45**, R6958 (1992).

[11] Y. Kayanuma, Phys. Rev. B **47**, 9940 (1993); Phys. Rev. A **50**, 843 (1994); Y. Kayanuma and S. Fukuchi, J. Phys. B **18**, 4089 (1985).

[12] S. Raghavan, V.M. Kenkre, D.H. Dunlap, A.R. Bishop, and M.I. Salkola, Phys. Rev. A **54**, R1781 (1996); D.H. Dunlap and V.M. Kenkre, Phys. Rev. B **34**, 3625 (1986).

[13] B.M. Garraway and S. Stenholm, Phys. Rev. A **45**, 364 (1992).

[14] G.S. Agarwal and W. Harshawardhan, Phys. Rev. A **50**, R4465 (1994).

[15] N.V. Vitanov and B.M. Garraway, Phys. Rev. A **53**, 4288 (1996).

[16] *Handbook of Mathematical Functions*, edited by M. Abramowitz and I.A. Stegun (Dover, New York, 1964).

[17] N.V. Vitanov and S. Stenholm, Phys. Rev. A **55**, 648 (1997).

[18] K. Mullen, E. Ben-Jacob, Y. Gefen, and Z. Schuss, Phys. Rev. Lett. **62**, 2543 (1989).

[19] N.V. Vitanov and P.L. Knight, J. Phys. B **28**, 1905 (1995).

[20] J.E. Golub and T.W. Mossberg, Phys. Rev. Lett. **59**, 2149 (1987).

[21] See D. Bouwmeester, G.P. Karman, N.H. Dekker, C.A. Schrama, and J.P. Woerdman, J. Mod. Opt. **43**, 2087 (1996), and references therein.

[22] N.V. Vitanov and P.L. Knight, Phys. Rev. A **52**, 2245 (1995).

[23] A. Erdélyi, W. Magnus, F. Oberhettinger, and F. G. Tricomi, *Higher Transcendental Functions* (McGraw-Hill, New York, 1953), Chap. VIII.